High-Resolution Atomic Force Microscopy Studies of the *Escherichia coli* Outer Membrane: Structural Basis for Permeability

Nabil A. Amro, Lakshmi P. Kotra, Kapila Wadu-Mesthrige, Alexy Bulychev, Shahriar Mobashery,* and Gang-yu Liu*

Department of Chemistry, Wayne State University, Detroit, Michigan 48202

Received July 27, 1999. In Final Form: November 8, 1999

The structural basis of the outer membrane permeability for the bacterium *Escherichia coli* is studied by atomic force microscopy (AFM) in conjunction with biochemical treatment and analysis. The surface of the bacterium is visualized with unprecedented detail at 50 and 5 Å lateral and vertical resolutions, respectively. The AFM images reveal that the outer membrane of native *E. coli* exhibits protrusions that correspond to patches of lipopolysaccharide (LPS) containing hundreds to thousands of LPS molecules. The packing of the nearest neighbor patches is tight, and as such the LPS layer provides an effective permeability barrier for the Gram-negative bacteria. Treatment with 50 mM EDTA results in the release of LPS molecules from the boundaries of some patches. Further metal depletion produces many irregularly shaped pits at the outer membrane, which is the consequence of progressive release of LPS molecules and membrane proteins. The EDTA-treated cells were analyzed for metal content and for their reactivities toward lysozyme and antibodies specific for LPS. The experiments collectively indicate that the metal depletion procedure did not remove all the LPS molecules despite a dramatic decrease in the metal content. The remaining LPS molecules are present outside the pits, whereas the bottom of the pits is devoid of these molecules. This new structure for the outer membrane exhibits higher permeability than that for the native cells.

Introduction

Gram-negative bacteria possess an outer membrane outside the peptidoglycan layer which is lacking in Gram-positive organisms. The essential function of the outer membrane is to serve as a selective permeability barrier, protecting bacteria from harmful agents such as detergents, drugs, toxins, and degradative enzymes. However, nutrients do penetrate to sustain bacterial growth. The structure and chemical composition of the outer membrane of one bacterium, *Escherichia coli*, has been studied extensively.[1−4] On the basis of previous understanding,[5] a schematic model of the *E. coli* outer membrane is shown in Figure 1. The lipid bilayer is asymmetric: the inner leaflet mostly contains close-packed phospholipid chains, while the outer leaflet is composed of the lipopolysaccharide (LPS) molecules.[1,4] It has been estimated that approximately 3.5 million molecules of LPS cover three-quarters of the surface of *E. coli*, with the remaining quarter being composed of membrane proteins.[5,6] The chemical composition of LPS molecules is known, as illustrated in Figure 1.[5−9] Each LPS molecule consists of *O*-antigens at the terminal, followed by outer core and inner core portions. The inner core is anchored to lipid A. Both the outer core and *O*-antigen regions contain carbohydrates, while the inner core region and lipid A of the LPS assembly incorporate various functionalities such as esters, phosphate esters, alcohols, aminoethyl phosphates, amines, and carboxylates.[5]

The LPS layer of the outer membrane plays an essential role in providing a selective permeability barrier for *E. coli* and other Gram-negative bacteria.[5,6,10] The evidence comes from both genetic and chemical experiments.[6,11,12] Mutants with altered LPS structures have increased permeability compared with that of native cells.[6,11,12,13] Ethylenediaminetetraacetate disodium (EDTA) was used first in 1958 to disrupt the LPS assembly and increase the permeability of bacteria cells.[14] From these earlier observations, it was inferred that the permeability depends on the density and the organization of the LPS molecules and lipoproteins.[1] However, it was difficult to extract the underlying mechanism or to directly correlate the molecular or even nanoscopic level structures with the observed permeability changes because of the lack of high-resolution techniques for structure characterization.

Since its invention in 1986,[15] AFM has been used more and more extensively to probe biosystems such as eukaryotic cells,[16] bacteria,[17−20] and viruses,[21−23] because

(1) Nikaido, H.; Vaara, M. *Microbiol. Rev.* **1985**, *49*, 1−32.
(2) Silva, M. T.; Sousa, J. C. F. *J. Bacteriol.* **1973**, *113*, 953−962.
(3) Lugtenberg, B.; Alphen, L. V. *Biochim. Biophys. Acta* **1982**, *737*, 51−115.
(4) Vaara, M. *Microbiol. Rev.* **1992**, *56*, 395−411.
(5) Raetz, C. R. H. *Annu. Rev. Biochem.* **1990**, *59*, 129−170.
(6) Rietschel, E. T.; Kirikae, T.; Schade, F. U.; Mamat, U.; Schmidt, G.; Loppnow, H.; Ulmer, A. J.; Zahringer, U.; Seydel, U.; Di-Padova, F.; Schreir, M.; Brade, H. *FASEB J.* **1994**, *8*, 217−225.
(7) Holst, O.; Brade, H. In *Bacterial endotoxic lipopolysaccharides*; Ryan, J. L., Brade, H., Eds.; CRC Press: Boca Raton, Fl, 1992; Vol. II, pp 135−170.
(8) Kusumoto, S. In *Bacterial endotoxic lipopolysaccharides*; Morrison, D. C., Ryan, J. L., Eds.; CRC Press: Boca Raton, Fl, 1992; Vol. I, pp 81−106.
(9) Raetz, C. R. H. *J. Bacteriol.* **1993**, *175*, 5745−5753.
(10) Leive, L. *Ann. NY Acad. Sci.* **1974**, *235*, 109−129.
(11) Raetz, C. R. H. In *Escherichia coli and Salmonella*: *Cellular and Molecular Biology*; Neidhart, F. C., Ed.; American Society for Microbiology: Washington, DC, 1996; Vol. I, pp 1035−1063.
(12) Nikaido, H. In *Membrane Transport and Information Storage. Advances in Membrane Fluidity*; Aloja, R. C., Curtain, C. C., Gordon, L. M., Eds.; Alan R. Liss, Inc.: New York, 1990; Vol. IV, pp 165−190.
(13) Chen, L.; Coleman, W. G. *J. Bacteriol.* **1993**, *175*, 2534−2540.
(14) McGregor, D. R.; Elliker, P. R. *Can. J. Microbiol.* **1958**, *4*, 494−499.
(15) Binning, G.; Quate, C. F.; Gerber, C. *Phys. Rev. Lett.* **1986**, *56*, 930−933.
(16) Hoh, J. H.; Hansma, P. K. *Trends Cell Biol.* **1992**, *2*, 208−213.
(17) Braga, P. C.; Ricci, D. *Antimicrob. Agents Chemother.* **1998**, *42*, 18−22.

10.1021/la991013x CCC: $19.00
Published on Web 01/19/2000

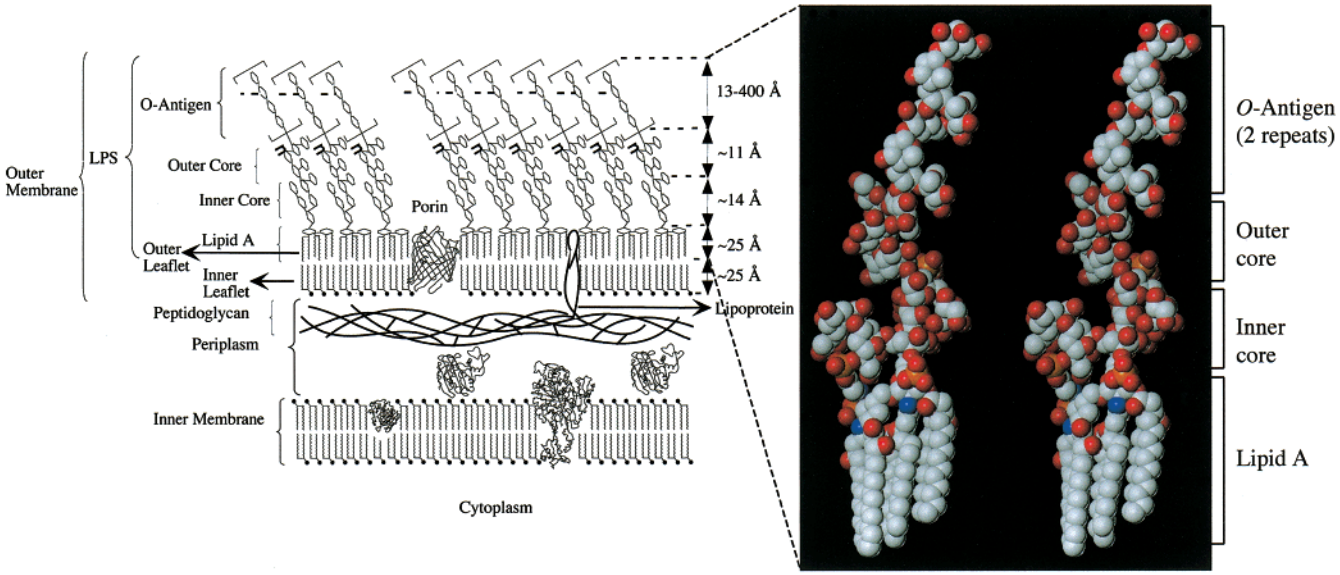

Figure 1. Schematic diagram of a portion of the cell envelop in Gram-negative bacteria. A stereoview of the model for a single LPS molecule with two repeats of *O*-antigen is displayed to the right. The model of the single LPS molecule was built using the Sybyl molecular modeling software (Tripos Associates, St. Louis, MO), and it was energy-minimized using the Tripos force field available in Sybyl. The atoms in the LPS molecule are coded according to atom type: white for carbon, red for oxygen, blue for nitrogen, and orange for phosphorus. Hydrogens are not shown for clarity of presentation.

AFM images can reveal structural details with unprecedented resolution. While optical microscopes are limited by diffraction ($\lambda/2$), AFM can achieve molecular and even atomic resolution for many materials.[24−28] In addition, three-dimensional (3D) information can be extracted directly from AFM topographic images. More importantly, AFM images can be acquired in liquid medium, a fact that makes this technique more advantageous in imaging living entities than electron microscopies. Furthermore, the operation of AFM is simpler, more convenient, and less costly than scanning electron microscopy (SEM) and transmission electron microscopy (TEM), which require an ultrahigh vacuum environment.[29]

In the present study, we have used atomic force microscopy to visualize the surface of both the native and structurally altered *E. coli*. We have brought to bear a number of techniques in conjunction with AFM imaging to determine the functionalities of the bacterial surface. Our study reveals the *E. coli* surface structure with unprecedented detail and brings us closer to understanding the structural basis for bacteria permeability and the organization of the surface components of Gram-negative bacteria in general.

Experimental Section

Bacterial Preparation. *Escherichia coli* JM109(pSF815A) was grown to mid-log phase in Terrific Broth (Difco Laboratories; 10 mL) at 37 °C for 7 h in the presence of 50 μg/mL kanamycin A. The final bacterial concentration is approximately (5−9) × 10^9 cells/mL. Bacterial concentrations were determined by measuring the absorbence of the culture at 600 nm ($0.1 \times O.D._{600} = 10^8$ cells/mL) in a spectrophotometer (HP 8453 diode array UV−visible spectrophotometer). Stock cultures of *E. coli* JM109(pSF815A) were maintained at −80 °C.

Metal Depletion from Bacterial Membrane. After growth, bacteria were centrifuged at 3000*g* for 2 min, and the wet pellet was resuspended in distilled water and was recentrifuged at 3000*g* for 2 min to remove the growth medium. The bacterial pellet was resuspended in either a 50 or a 100 mM EDTA solution (1 mL) in water (pH adjusted to 8.0 using a 0.1 M NaOH solution). The suspension was incubated for 40 min at 37 °C with gentle shaking. Bacteria were pelleted by centrifugation at 3000*g* for 2 min, resuspended in water, and recentrifuged (2×), and the final pellet was again suspended in distilled water (1 mL) for analysis.

Analysis of Metal Content. The EDTA solutions (100 mM) from the metal-depletion experiments were analyzed for metal content by Ricerca, Inc. (Painesville, OH), using inductively coupled plasma-atomic emission spectrometry (ICP-AES). The analysis was performed for 30 different metals (in groups I and II and transition metals) and for phosphorus, sulfur, and boron. The standard deviation for those elements present in the mixture in excess of 10% was ±2%, and it was much higher for elements present at <0.1%.

Spheroplast Preparation. The procedure for spheroplast preparation was adapted from the protocol by Epicenter Technologies, Madison, Wisconsin.[30] Lysozyme from chicken egg white (95% Grade-I, Sigma Chemical Company; 0.91 mg) was dissolved in 1.5 mL of 0.2 M HEPES buffer, pH 7.5. A 75 μL portion of the above lysozyme solution (30 000 units/mL) was added to 1.5 mL of the *E. coli* solution (7.5×10^7 cells). The mixture was incubated for 5 min at room temperature, followed by an additional 5 min at 4 °C. The suspension was centrifuged at 1000*g* for 2 min, the pellet was resuspended in water (1 mL) and was recentrifuged

(18) Rajyaguru, J. M.; Kado, M.; Richardson, M. C.; Muszynski, M. J. *Biophys. J.* **1997**, *72*, 1521−1526.
(19) Razatos, A.; Ong, Y.-L.; Sharma, M. M.; Georgiou, G. *Proc. Natl. Acad. Sci. U.S.A.* **1998**, *95*, 11059−11064.
(20) Umeda, A.; Saito, M.; Amako, K. *Microbiol. Immunol.* **1998**, *42*, 159−164.
(21) Drygin, Y. F.; Bordunova, O. A.; Gallyamov, M. O.; Yaminsky, I. V. *FEBS Lett.* **1998**, *425*, 217−221.
(22) Ohnesorge, F. M.; Horber, J. K.; Haberle, W.; Czerny, C. P.; Smith, D. P.; Binnig, G. *Biophys. J.* **1997**, *73*, 2183−2194.
(23) Wadu-Mesthrige, K.; Pati, B.; McClain, W. M.; Liu, G. Y. *Langmuir* **1996**, *12*, 3511−3515.
(24) Liu, G. Y.; Salmeron, M. B. *Langmuir* **1994**, *10*, 367−370.
(25) Butt, H.-J.; Seifert, K.; Bamberg, E. *J. Phys. Chem.* **1993**, *97*, 7316−7320.
(26) Miura, K.; Shukuya, Y. *Jpn. J. Appl. Phys.* **1993**, *32*, 4752−4753.
(27) Xu, S.; Laibinis, P. E.; Liu, G.-Y. *J. Am. Chem. Soc.* **1998**, *120*, 9356−9361.
(28) Kolbe, W. F.; Ogletree, D. F.; Salmeron, M. *Ultramicroscopy* (*North-Holland, Amsterdam*) **1992**, *42−44*, 1113−1116.
(29) *Scanning Electron Microscopy and X-ray Microanalysis*, 2nd ed.; Goldstein, J. I., Neubury, D. E., Echlin, P., Joy, D. C., Roming, A. D., Jr., Lyman, C. E., Fiori, C., Lufshin, E., Eds.; Plenum Press: New York, 1992; pp 1−270.
(30) Neu, H. C.; Heppel, L. A. *J. Biol. Chem.* **1965**, *240*, 3685−3692.

(2×), and the final pellet was resuspended in distilled water (1 mL) for analysis.

Antibody Treatment. A suspension of *E. coli*, native or metal-depleted (~10^8 cells in 2 mL), was incubated with polyclonal rabbit anti-*E. coli* lipopolysaccharide antibody (primary antibody, IgG stock concentration 1 mg/mL; Biodesign International, 1:80 000 dilution, final volume 400 μL) at 4 °C for 30 min in a 10 mM NaCl solution. These cells were centrifuged at 3000*g* for 2 min and resuspended in distilled water (2×) prior to the AFM experiments.

For fluorescence microscopy studies, native and metal-depleted *E. coli* and *Bacillus subtilis* BD170(pSF815A) were treated with the antibody as described above. *B. subtilis* BD170(pSF815A) was grown on VL (Difco) medium in the presence of 25 μg/mL kanamycin A for 20 h at 37 °C. Cells were washed similarly and reconstituted by the addition of 40 μL of a 10 mM solution of NaCl to give a final concentration of 9.0×10^8 cells/mL. All four samples (40 μL each) were diluted by the addition of an equal volume of 10 mM NaCl to result in 80 μL of cellular suspension with the final cell concentration of 4.5×10^8 cells/mL. The primary antibody solution (5 μL) was added to each of the samples, and they were incubated at ice−water temperature for 30 min. These cells were centrifuged at 3000*g* for 2 min and washed once with deionized water to remove the unbound antibodies. Subsequently, fluorescein isothyocyanate (FITC)-conjugated goat anti-rabbit IgG (secondary antibody, Biodesign International, Kennebunk, ME; 5 μL) was added to each sample to a final concentration of 120 μg/mL. Secondary antibody was labeled with the fluorescent tag FITC, which allowed visualization by fluorescence microscopy. The samples were incubated for an additional 30 min at ice−water temperature. The labeled cells were centrifuged at 3000*g* for 2 min, resuspended in 10 mM NaCl, and centrifuged (2×). Finally, the pellet was suspended in deionized water (90 μL) for study.

Fluorescence Microscopy. The presence of LPS at the outer membrane can be investigated using fluorescence microscopy. Three *E. coli* samples, the native bacteria and cells treated with 50 and 100 mM EDTA solutions, respectively, were imaged. *B. subtilis*, a Gram-positive bacterium, served as a negative control (blank) because it lacks the LPS layer. The bacteria were first tagged by fluorescence active antibodies, followed by the procedures described above. These cells were then deposited onto a glass slide and examined using a Carl Zeiss fluorescence microscope (Batavia, IL) with mercury illumination interfaced to a Perceptics Biovision System (Knoxville, TN). A narrow bandpath discriminating filter set was used to allow excitation at 485/22 nm and emission at 530/3 nm (Omega Optical, Bratleboro, VT). The cell-associated FITC fluorescence levels were quantified using a photomultiplier tube system (Photochemical Research Associates, Inc., London, Ontario, Canada). An average of fluorescence for 50 randomly selected cells was used in each trial.

Atomic Force Microscopy. The instrument is a state-of-the-art microscope constructed in house. It can operate under ambient laboratory conditions, in a vacuum or in solution.[28,31] The cantilevers were standard microlevers from Digital Instrument with a force constant of 0.38 N/m. The scanning head incorporates a deflection type configuration with a quadrant photodiode detector that allows simultaneous acquisition of both topographic and frictional force images.

The drop-and-dry method was used to transfer bacteria from solution to a solid support for AFM studies. To study structural features of individual cells, we used a submonolayer coverage. For each specimen, 20 μL of bacterial solution (total number of cells ~9×10^6) was placed on a 1 cm^2 glass slide (thickness 0.5 mm). To enhance the adhesion, the glass slide was pretreated with the Piranha solution (1:3 ratio of 30% H_2O_2/concentrated H_2SO_4) and washed copiously with deionized water before introduction of the bacteria. The surface was then washed with distilled water (40 μL, 3×) and allowed to dry in air.

To study the structure of the *E. coli* cell membrane after the various modifications described above, we quenched the reactions using the centrifugation-and-washing cycle described previously. The cells were immediately imaged in 2-butanol to preserve their original structures. This is analogous to the "freeze-and-look" method used for kinetics studies. Ideally, it is desirable to obtain the images in an aqueous suspension to mimic the native environment. The images acquired in aqueous media show very similar morphologies, but lower resolution in comparison with that of images taken in 2-butanol. This is because the adhesive forces between the AFM tip and *E. coli* measured in water were high (1.74 nN or higher), which made it difficult to resolve detailed structures. In contrast, imaging in 2-butanol effectively eliminates the capillary interaction between the tip and the surface and allows images to be taken at low imaging forces (0.4 nN). The gentle tip−surface interaction reduces adhesion and surface deformation, thus resulting in high spatial resolution.

Results and Discussions

Structural Changes of the Outer Membrane during the Metal Depletion Process. It is known from previous studies that EDTA treatment can increase the permeability of the outer membrane of *E. coli*.[1,3,4] Higher EDTA concentrations and/or longer incubation times lead to more profound effects, and prolonged treatment can result in the death of bacteria through the rupture of the cellular envelope.[10,32,33] It has been proposed that EDTA extracts divalent metal ions such as Ca^{2+} and Mg^{2+} from their binding sites within the outer membrane, weakening the LPS interactions and causing the release of a significant portion of LPS and proteins from the bacterium.[10,32−35] These changes on the bacterial surface lead to increased permeability. However, more detailed structural changes at the outer membrane and the molecular mechanism of the permeability increase are still unknown. The remaining issues include the nature of the packing of the LPS molecules and the extent and the precise locations of outer membrane components released upon metal depletion. In this study, we have visualized the detailed features of the *E. coli* surface using AFM. We have compared the AFM images acquired for the native cells and for cells after partial (using a 50 mM EDTA solution) and nearly complete metal depletion (using a 100 mM EDTA solution).

The extraction of metal ions from *E. coli* was investigated using ICP-AES to measure the metal content in the EDTA solution after reacting with *E. coli*. Three metal elements were detected: Mg^{2+}, Ca^{2+}, and Fe^{2+} at the concentrations 57%, 41%, and 2% of the total metal content, respectively. The EDTA solution prior to the treatment did not contain these three ions. These elemental analyses confirm the previous reports that extended EDTA treatment has extracted divalent metal ions from the outer membrane.[34−38]

A large scan area (15×15 μm^2) was first made for the native *E. coli* JM109(pSF815A) in order to select the desired cells for higher-resolution imaging. As shown in Figure 2A, individual bacteria are readily distinguishable. The typical length of the bacterial cell is 2−6 μm, consistent with previously reported values.[17−20] The corresponding cursor profile reveals that the measured width and height of *E. coli* are 1.1 ± 0.1 and 0.8 ± 0.1 μm, respectively. The

(31) Liu, G. Y.; Fenter, P.; Chidsey, C. E. D.; Ogletree, D. F.; Eisenberger, P.; Salmeron, M. *J. Chem. Phys.* **1994**, *101*, 4301−4306.
(32) Leive, L. *Proc. Natl. Acad. Sci. U.S.A.* **1965**, *53*, 745−750.
(33) Bayer, M. E.; Leive, L. *J. Bacteriol.* **1977**, *130*, 1364−1381.
(34) Coughlin, R. T.; Tonsager, S.; McGroarty, E. J. *Biochemistry* **1983**, *22*, 2002−2007.
(35) Ferris, F. G.; Beverdge, T. J. *Can. J. Microbiol.* **1986**, *32*, 594−601.
(36) Schindler, M.; Osborn, M. J. *Biochemistry* **1979**, *18*, 4425−4430.
(37) Stinnett, J. D.; Gilleland, H. E.; Eagon, R. G. *J. Bacteriol.* **1973**, *114*, 339−407.
(38) Coughlin, R. T.; Caldwell, C. R.; Haug, A.; McGroarty, E. J. *Biochem. Biophys. Res. Commun.* **1981**, *100*, 1137−1142.

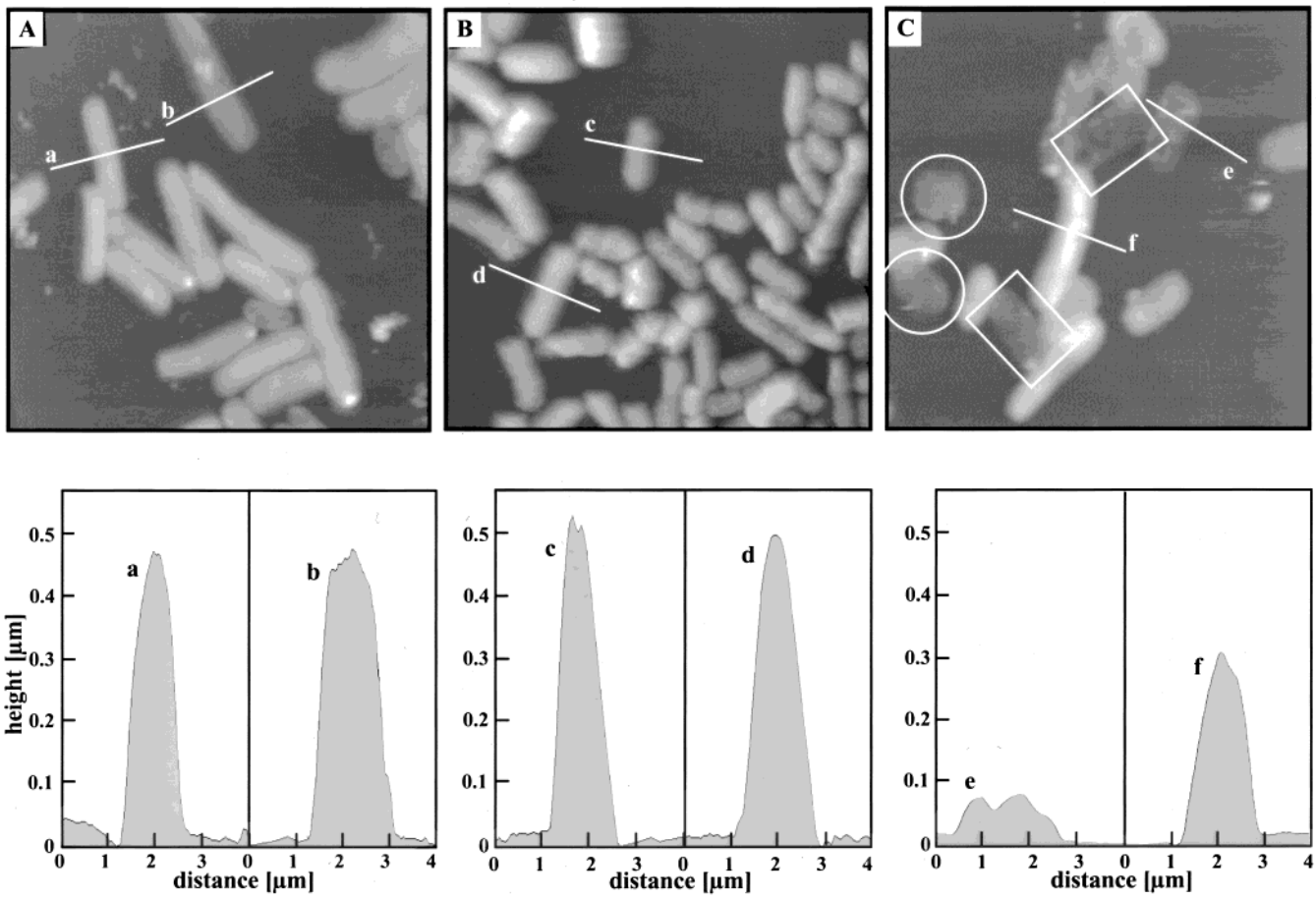

Figure 2. Topographic images of the native *E. coli* JM109(pSF815A) (left) and cells treated with 50 mM (middle) and 100 mM (right) EDTA solutions. The total scan area is 15 × 15 μm^2.

apparent width may be slightly wider than the actual width due to tip convolution.[39−41] The detailed structure of the cell membrane has been studied by systematically zooming in on desired cells and regions within the cell envelope. An example is shown in Figure 3A and B. While it is technically not possible at the present to resolve individual LPS molecules using AFM, the images shown in Figure 3 represent the highest resolution available and reveal many detailed structural features of the outer membrane of *E. coli*. The vertical and lateral resolutions of the AFM images shown in Figure 3 are approximately 5 and 50 Å, respectively, which are estimated from the smallest features resolved. While previous studies using optical microscopy indicate the surface of the native *E. coli* to be smooth,[42,43] AFM images (Figure 3B and C) clearly reveal that the surface of *E. coli* is rough at nanometer resolution. The outer membrane exhibits protrusions ("bumps") with lateral dimensions of 250−600 Å and a surface roughness of 22−90 Å.

According to the lateral dimensions of the bumps measured by AFM and the chemical structure of one LPS molecule (see Figure 1), each patch contains approximately 600 to 3500 LPS molecules. The difference in the heights of the bumps is most likely due to the different numbers of *O*-antigen units (2 to 40) at the termini of the LPS molecules. Another factor contributing to our observed surface roughness is the nanoscopic curvature of the *E. coli* outer membrane, 20−40 nm in diameter, as first revealed in electron micrographs.[44−46] The packing of the nearest neighbor LPS patches is tight, and as such the LPS surface provides an effective permeability barrier for the Gram-negative bacteria. The presence of the patches and local curvatures have advantages over perfectly packed and smooth LPS layers, because of higher mechanical stability. From micromechanics, a layer of a molecular assembly consisting of local clusters and curvatures can resist, accommodate, and heal a local structural perturbation much more readily than a smooth and defect-free assembly. Dark features are observed in Figure 3B and C, representing the void spaces between the LPS patches. The opening of these dents ranges from 250 to 600 Å with depths of 25−85 Å. The actual opening and depth of these dents are likely to be larger than our measured values because the AFM tip cannot always reach the bottom of the depressions. Since it is known that ∼25% of the outer membrane is made up of proteins, it is tempting to conclude that these depressions may be caused by the presence of membrane proteins. Further investigations of the released contents are necessary to confirm this hypothesis.

(39) The apparent width here may be larger than the actual value due to tip convolution, as discussed in ref 39−41. Ramirez-Agilar, K. A.; Rowlen, K. L. *Langmuir* **1998**, *14*, 2562−2566.
(40) Markiewicz, P.; Goh, M. C. *Rev. Sci. Instrum.* **1995**, *66*, 3186−3190.
(41) Keller, D.; Frank, F. S. *Surf. Sci.* **1993**, *294*, 409−419.
(42) Sun, Q.; Margolin, W. *J. Bacteriol.* **1998**, *180*, 2050−2056.
(43) Eynard, N.; Sixou, S.; Duran, N.; Teissie, J. *Eur. J. Biochem.* **1992**, *209*, 431−436.
(44) Stock, J. B.; Rauch, B.; Roseman, S. *J. Biol. Chem.* **1977**, *252*, 7850−7861.
(45) Kadurugamuwa, J. L.; Beveridge, T. J. *J. Antimicrob. Chemother.* **1997**, *40*, 615−621.
(46) Fujimoto, S.; Meno, Y.; Horikawa, K. *Microbiol. Immunol.* **1998**, *42*, 527−531.

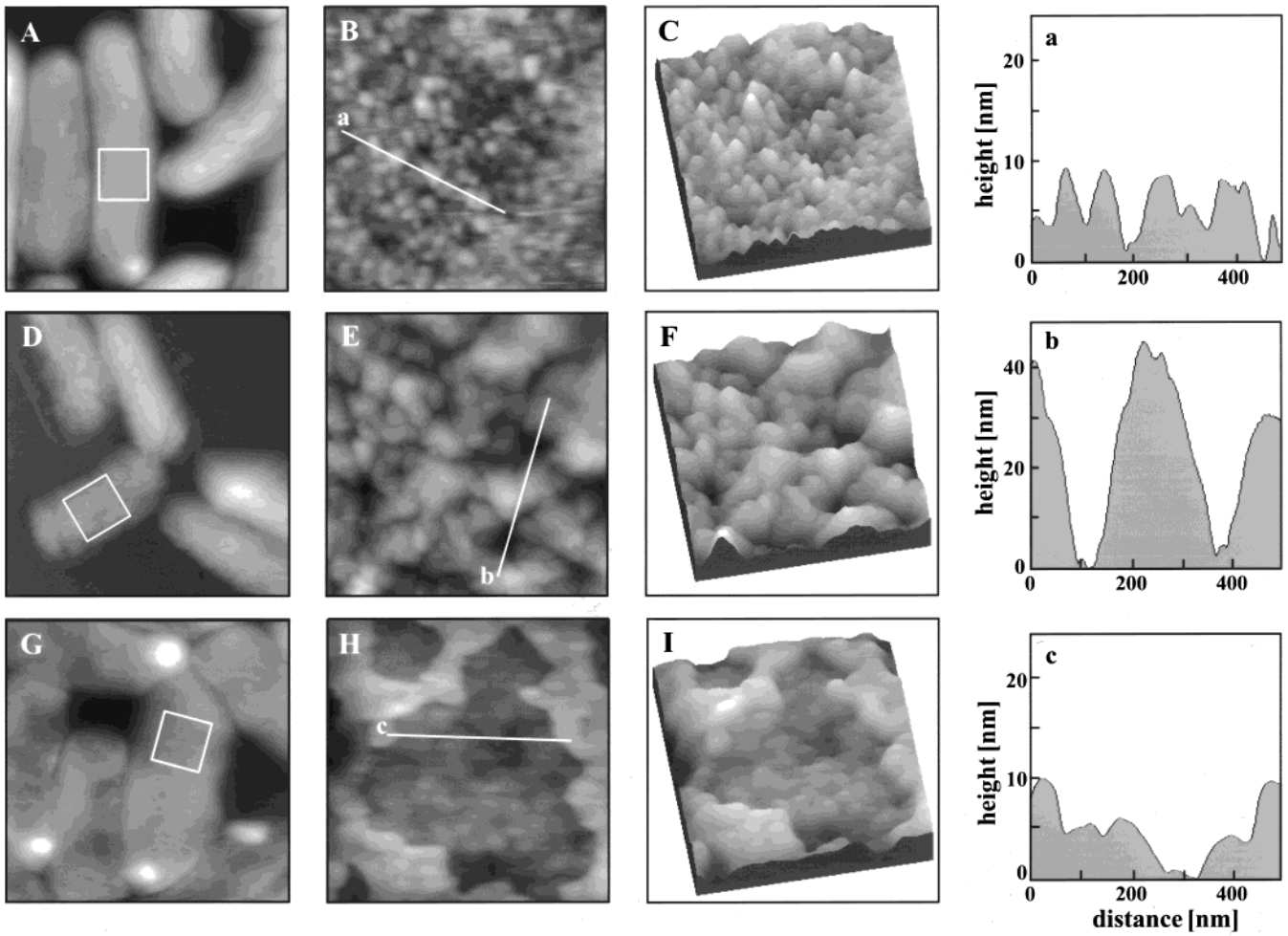

Figure 3. AFM studies of the native *E. coli* JM109(pSF815A) (top row) and cells treated with 50 mM (middle row) and 100 mM EDTA (bottom row). Images of entire bacteria are shown in the left column (total scanning area $4 \times 4\ \mu m^2$). Images acquired by zooming into the boxed areas are displayed in the second (two-dimensional) and third (three-dimensional) columns (total scanning area $0.8 \times 0.8\ \mu m^2$). The corresponding cursor profiles (right column) provide quantitative measurements of the dimensions for the surface features.

The initial metal depletion was accomplished by soaking the native bacteria in a 50 mM EDTA solution for 40 min at 37 °C. The three-dimensional structure (height and width) of the individual cells remained unchanged, as shown in the large area topographic images in Figure 2B. The higher-resolution topographic images in Figure 3D−F, however, reveal a profound change in LPS packing. The surface of *E. coli* becomes much rougher than that for the native bacterium, as shown in the second row in Figure 3. The corresponding cursor profiles reveal higher bumps and deeper dents present on the modified cell membrane. The protrusions in images 3E and F have apparent heights from 250 to 450 Å. The experiments shown in Figure 3 were carried out ex situ; for example, images 3B, E, and H were acquired from different cells. To verify the observed changes in surface structure and roughness shown in Figure 3, we have imaged and compared over 50 high-resolution images, and the results are consistent. The increase in surface roughness is attributed to the release of LPS molecules from boundaries of some patches. With LPS aggregates more separated, the AFM tip can probe deeper into the membrane, resulting in the observed morphological changes in the outer membrane. We estimated ~13% of the LPSs were detached from the cell membrane, on the basis of the average surface roughness and tip convolution.[39−41]

Further depletion of metal was accomplished by soaking the native bacteria in a 100 mM EDTA solution for 40 min at 37 °C. While most of the bacteria still preserve their cylindrical shape, their heights decrease by 40% relative to those of the native cells. The rod-shape morphology of *E. coli* is governed by the cross-linked peptidoglycan (cell wall). The decrease in the height indicates a partial release of the cytoplasmic content. About 2−10% of cells exhibited more severe damage. Figure 2C includes two cylindrically shaped, completely flattened and emptied cells (within the rectangular frames in Figure 2C) and a disklike cell (within the circular frame in Figure 2C). The former is most likely caused by a gradual release of most of the cytoplasmic content because the shape was maintained, and the latter represents a lysis of bacteria during the treatment.

For those cells that maintain their rod-shaped morphology, the high-resolution images shown in both Figure 3 (bottom row) and Figure 4 reveal that metal depletion has altered the structure of the outer membrane dramatically. After treatment with 100 mM EDTA, the outer membrane has a new and distinct feature: appearance of many shallow pits with openings from 400 to 7000 Å. These pits are irregularly shaped and have an average depth of 63 Å (±13 Å). The largest pit (7000 Å wide) in Figure 3H is shown in more detail in Figure 4. The bottom of the pit is smoother than the surfaces of the elevated areas and exhibits a hole with an apparent depth of 27 ± 7 Å (cursor a) and a diameter of 1600 ± 100 Å. The observed morphological changes are due to cells' reaction with EDTA

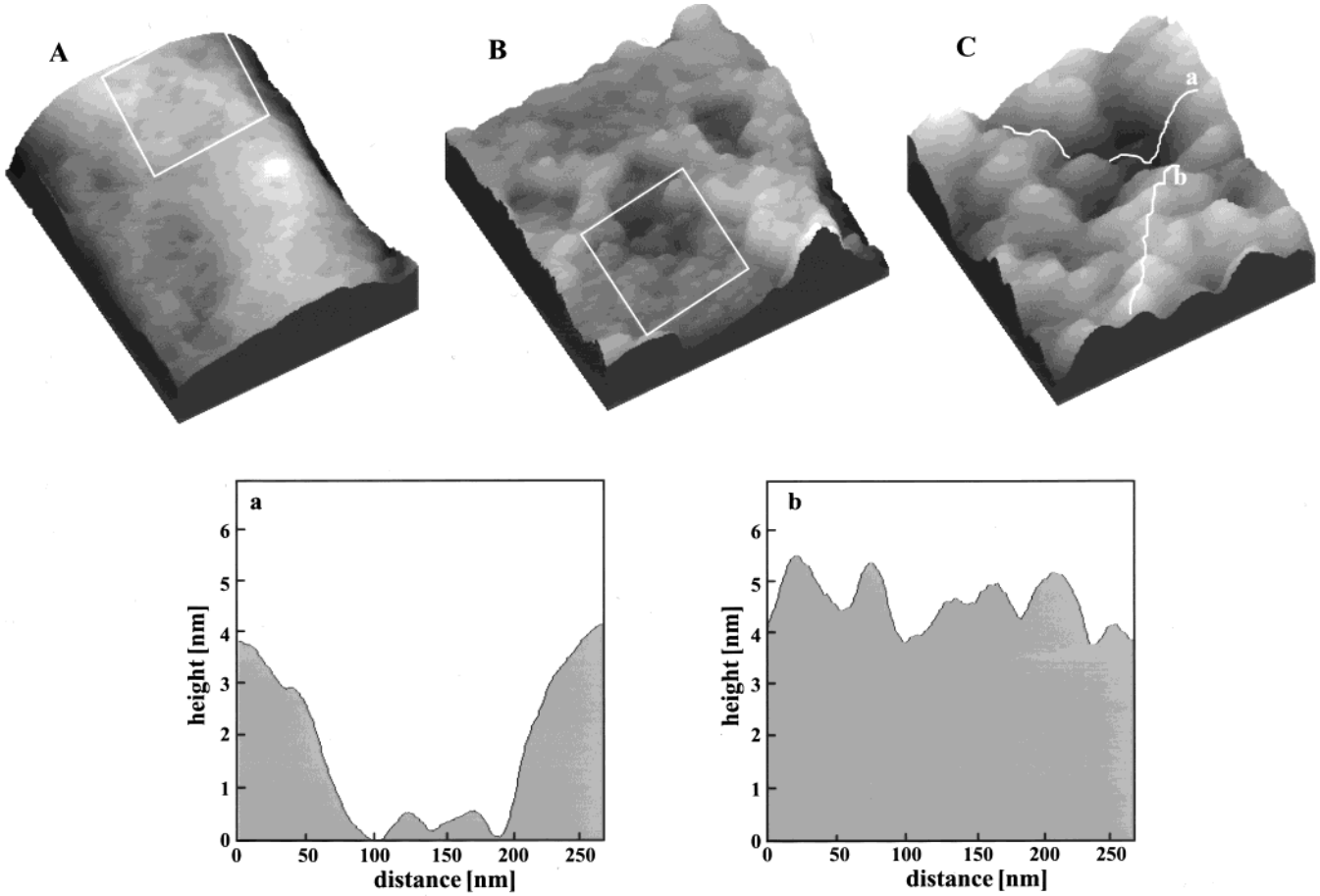

Figure 4. Topographic AFM images of *E. coli* JM109(pSF815A) after metal depletion. Images A, B, and C are the progressively expanded views of the chosen regions with scanning areas of 1.90 × 2.37 μm^2, 1 × 1 μm^2, and 0.38 × 0.38 μm^2, respectively. The high-resolution image shown in panel C reveals the detailed surface features at the bottom of the pits. The cursor plots a and b provide a three-dimensional measurement of these structural features.

instead of the washing-and-centrifugation procedures, as these changes were not observed for cells subject to the same treatment in the absence of EDTA.

The appearance of pits indicates the release of outer membrane components, predominately LPSs and membrane proteins. The new structure is not as tight as that of the native cell, which leads to liberation of the periplasmic content. Our preliminary molecular dynamics simulations suggest that the absence of metals in the LPS assembly facilitates dissociation of LPS molecules from the assembly.[47] The metal depletion process does not remove all of the LPS molecules from the surface, as will be further confirmed later in this report.

From our high-resolution images, one can infer the following regarding the metal-depletion mechanism. The distribution of metal ions in the native *E. coli* is not uniform at the nanoscopic level due to the inhomogeneous structure of the outer membrane, such as the presence of membrane proteins, different sizes for patches of LPS, and local curvatures. Therefore, the liberation of metal is regional instead of uniform. After extraction of metal ions by EDTA, intermolecular interactions among LPSs within patches are weakened. Desorption of LPS occurs from the boundaries of these LPS patches, gradually leading to the release of entire patches and membrane proteins. The pits imaged in Figures 3 and 4 are likely the direct result of the regional release of membrane components after removal of metal ions. Another possibility is that pits are the results of reassembly of the remaining LPS molecules after the release of their neighbors. Higher resolution and in situ studies are necessary to reveal the metal-depletion mechanism at the molecular level and address the issue of whether the LPS molecules reassemble during the metal-depletion process.

Permeability and Functionality of the Outer Membrane. Previous studies have shown that after EDTA treatment the periplasm becomes permeable to the milieu.[1,4,10,32,33,48,49] The discussions in the previous section have shown that AFM images reveal the structural basis for the low permeability of the native *E. coli* and the increase in the cell permeability after metal depletion. After the 50 mM EDTA treatment, the three-dimensional structure (height and width) of an individual cell remains unchanged, as shown in the AFM images in Figure 2. While small molecules can enter the cells, the cytoplasmic contents still remain entrapped within the native organism. In contrast, further depletion of metal by 100 mM EDTA treatment resulted in a 40% decrease of the cell height (Figure 2), indicating the likely dehydration of bacterium in the 2-butanol medium after the outer membrane has been severely altered. The AFM imaging medium (2-butanol) is likely behaving as a dehydrant, similar to the case of sucrose treatment in dehydration of bacteria prior to liberation of the periplasmic content. We

(47) Kotra, L. P.; Golemi, D.; Amro, N. A.; Liu, G. Y.; Mobashery, S. *J. Am. Chem. Soc.* **1999,** *121*, 8707−8711.

(48) Pellegrini, A.; Thomas, U.; von Fellenberg, R.; Wild, P. *J. Appl. Bacteriol.* **1992**, *72*, 180−187.

(49) Wild, P.; Gabriel, A.; Schraner, E. M.; Pellegrini, A.; Thomas, U.; Frederick, P. M.; Stuart, M. C. A.; Fellenberg, A. V. *Microsc. Res. Tech.* **1997**, *39*, 297−304.

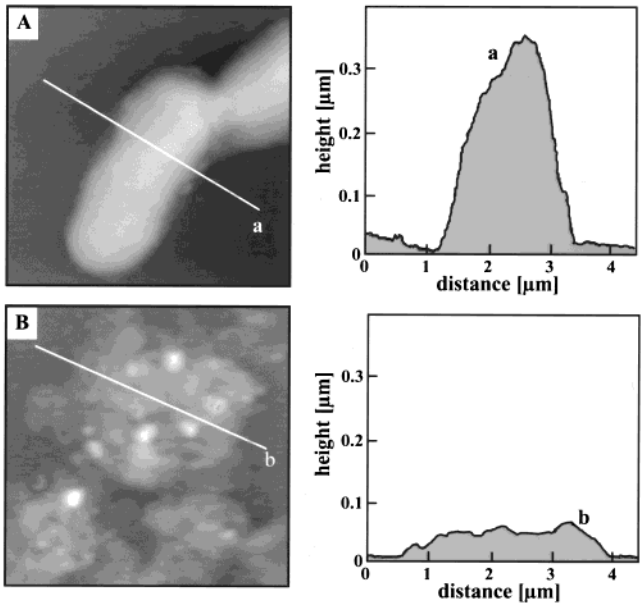

Figure 5. Topographic images of *E. coli* cells after reactions with lysozyme. Native *E. coli* JM109(pSF815A) (A) and 100 mM-treated cells (B) were used respectively for this treatment. The dimensions are given in the corresponding cursor profiles depicted to the right. The total scanning areas for the AFM images are 5 × 5 μm^2.

see more severe dehydration for the 100 mM EDTA-treated cells than for the native and 50 mM EDTA-treated cells.

The *E. coli* permeability can also be directly tested by imaging cells before and after lysozyme treatment. It is known that, without the permeability barrier, lysozyme can degrade the peptidoglycan.[48,49] Electron microscopy studies have shown that the degraded cells lost their cylindrical geometry.[50] Thus, the accessibility of lysozyme to the peptidoglycan is an indication of the permeability to the periplasma. Figure 5 compares cell morphology after lysozyme treatment. The topographic image in Figure 5A shows that the structure of the native cell is not affected by lysozyme, further demonstrating the efficiency of the LPS layer as a permeability barrier. However, the metal-depleted bacteria lost their original structure after reaction with lysozyme and became spheroplast (0.05 μm in thickness), as shown in Figure 5B. Such an observation is valid for the majority of cells we have investigated, typically 100 cells per AFM experiment. This is, to our knowledge, the first visualization of the *E. coli* spheroplast in three dimensions. The fact that lysozyme can degrade metal-depleted bacteria is a strong indication that certain areas of peptidoglycan are directly exposed after the 100 mM EDTA treatment.

It was proposed previously that EDTA treatment releases only a portion of the outer membrane.[10] This model is consistent with our AFM images shown in Figures 3 and 4, from which the positions and numbers of released LPS patches may be estimated. The area occupied by the pits makes up 40−50% of the cell surface, suggesting that at least 40−50% of the outer membrane contents is liberated. To further test if there are LPS molecules remaining at the outer membrane after metal depletion, we have investigated the reactivity of the bacterial surface with specific anti-LPS antibodies. Antibodies are large proteins of approximately 150 kDa. Each IgG molecule exhibits a Y-shaped geometry, with the dimensions 145 × 85 × 40 $Å^3$. Hence, they are easily visualized from topographic images due to the expected height increase when attached to cell surfaces (vide infra). After treatment with anti-LPS antibody, AFM study shows that the surface of the native *E. coli* was covered with essentially a monolayer of antibody molecules. For the metal-depleted cells, AFM images were acquired before and after the treatment with antibodies and shown in Figure 6. Similar to that of the native *E. coli*, the measured surface roughness is increased by 75 ± 45 Å after reaction with

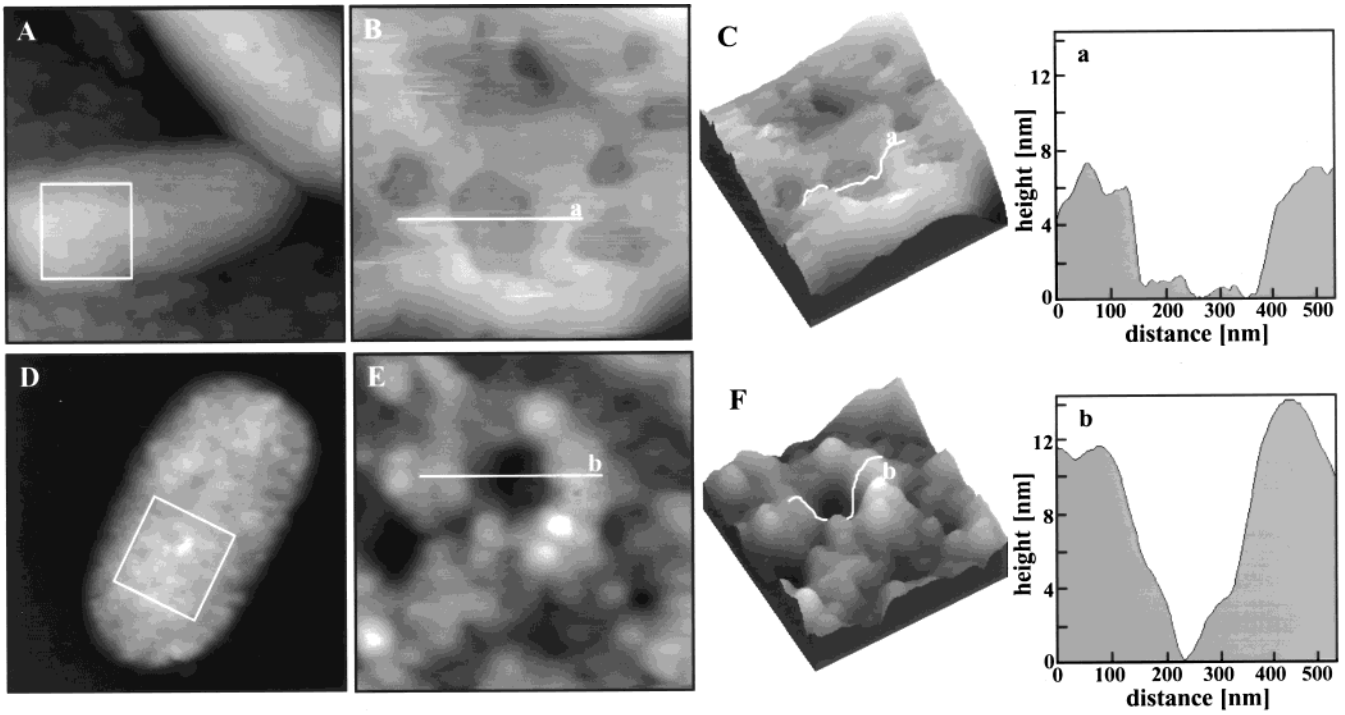

Figure 6. Topographic images of *E. coli* JM109(pSF815A) after metal depletion (top row) and then treatment with anti-LPS antibody (bottom row). The scanning areas are 3.5 × 3.5 and 1 × 1 μm^2 for the low- (left column) and high-resolution (second and third columns) images, respectively. The high-resolution images and corresponding cursor profiles clearly reveal the presence of antibody molecules outside the pits.

Table 1. Fluorescence Measurements after Tagging Bacteria with FITC-Labeled Antibody

sample	fluorescence intensity	
	K_{counts}	%[a]
native *E. coli* JM109(pSF815A)	246 ± 31	100
50 mM EDTA-treated *E. coli*	182 ± 14	74
100 mM EDTA-treated *E. coli*	103 ± 27	42
B. subtilis BD170(pSF815A)	24 ± 11	10

[a] The percentages are normalized according to the value for the native *E. coli*.

the anti-LPS antibody. The bright spots in images 6E and F correspond to individual antibody molecules according to the height measurements. The cursor profiles shown in Figure 6 indicate the heights of typical surface features prior to and after the antibody treatment. These AFM studies suggest the presence of some LPS molecules at the cell membrane. In contrast to the case of native *E. coli*, the decoration by antibody covers only 50% of the surface in the metal-depleted cells. As shown in images 6D and E, only the areas outside the pits react with antibody molecules. This observation confirms our earlier model that the areas outside the pits are the remaining LPS patches, while the bottoms of the pits are likely to be the exposed peptidoglycan polymers.

To further verify the presence of LPS after metal depletion, the *E. coli* cells were treated with conjugated goat anti-rabbit IgG secondary antibody with the fluorescence tag FITC. The labeling by the secondary antibody was characterized using fluorescence microscopy and is summarized in Table 1. Florescence microscopy revealed that the intensity of the fluorescence dropped as the concentration of EDTA was increased during the treatment of the *E. coli*. The decrease of the fluorescence intensity indicates the decrease of the LPS population upon EDTA treatment. The fact that we can still detect fluorescence indicates that there are remaining LPS patches after the metal-depletion processes.

Summary and Conclusions

Using AFM in conjunction with biochemical analyses, we have investigated the structural basis of the outer membrane permeability for the bacterium *E. coli*. The surface of the bacterium is visualized with unprecedented detail. Our AFM images clearly reveal that the surface of *E. coli* is not smooth at nanometer resolution due to the inhomogeneous packing of LPS and local curvatures. The outer membrane is predominately made of patches of LPS each containing hundreds to thousands of LPS molecules. The packing of the nearest neighbor patches is tight, and as such the LPS layer provides an effective permeability barrier for the Gram-negative bacteria.

Divalent metal ions play an important role in maintaining the assembly of the LPSs and membrane proteins within the outer membrane. It has been known since the 1960s that the liberation of the periplasmic contents of Gram-negative bacteria can be achieved by depletion of metals from the surface of these organisms.[1,3,4,10,34−38] It serves as a versatile technique to increase the cell permeability and the liberation of proteins that either are normally sequestered in the periplasma or are shuttled there by manipulation of protein secretion in biotechnology. We have provided insight for the first time into the mechanism by which this process takes place. Our AFM images reveal that LPS molecules are released from the boundaries of certain patches during the initial treatment by EDTA. Further metal depletion produces a very distinct structure at the outer membrane, which entails the appearance of irregularly shaped pits that make up 40−50% of the cell surface. The rest of the cell surface consists of the remaining LPS patches and membrane proteins. The pits are formed mainly as a result of liberation of LPS molecules and some membrane proteins, exposing areas of the peptidoglycan surface. An outer membrane with such a morphology exhibits a significant increase in permeability.

Our study has proven AFM to be a useful technique in providing structural information for biological organisms. AFM images allow structures of cell membranes to be visualized with unprecedented resolution. In addition, three-dimensional information can be extracted from the topographic images. Work is in progress to improve the resolution in aqueous media and image cell growth and its biochemical reactions in situ and under near physiological conditions.

Acknowledgment. We appreciate many helpful discussions with Professors James Geiger and Estelle McGroarty at Michigan State University. The authors acknowledge Andrew Kindzelskii for his help with the fluorescence microscopy experiment and Eduardo Azucena for his help in preparation of the bacteria. G.-y.L. thanks the Arnold and Mable Beckman Foundation for a Young Investigation Award.

LA991013X

(50) Bernard, E. F.; Hase, T. *Scanning Microsc.* **1991**, *5*, 595−599.